Heliyon 9 (2023) e19396

Contents lists available at ScienceDirect

Heliyon

journal homepage: www.cell.com/heliyon

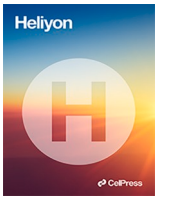

Electroacupuncture preconditioning protects against myocardial ischemia-reperfusion injury by modulating dynamic inflammatory response

Hua Bai [a,b,1], Sen-Lei Xu [a,b,1], Jun-Jing Shi [a,b], Ya-Ping Ding [a,b], Qiong-Qiong Liu [a,b], Chun-Hong Jiang [a,b], Li-Li He [a,b], Hong-Ru Zhang [c], Sheng-Feng Lu [a,d,*], Yi-Huang Gu [a,b,**]

[a] *Key Laboratory of Acupuncture and Medicine Research of Ministry of Education, Nanjing University of Chinese Medicine, Nanjing, 210023, China*
[b] *Acupuncture and Tuina College, Nanjing University of Chinese Medicine, Nanjing, 210023, China*
[c] *School of Medicine & Holistic Integrative Medicine, Nanjing University of Chinese Medicine, Nanjing, 210023, China*
[d] *School of Elderly Care Services and Management, Nanjing University of Chinese Medicine, Nanjing, 210023, China*

ARTICLE INFO

Keywords:
Electroacupuncture preconditioning
myocardial ischemia-reperfusion injury
NLRP3 inflammasome
Dynamic inflammatory response

ABSTRACT

Background: The protective effects of electroacupuncture (EA) preconditioning against myocardial ischemia-reperfusion injury (MIRI) have been reported. However, the underlying mechanism remains unclear. Recent research has indicated that the dynamic inflammatory response following MIRI plays an essential role in the progression of myocardial injury. This study aimed to investigate the myocardial protective effects of EA preconditioning on MIRI in rats and to explore the relevant mechanism from the perspective of dynamic inflammatory response.

Methods: A MIRI model was employed, and the rats were subjected to EA on Neiguan for four days prior to modeling. The myocardial protective effect of EA preconditioning was evaluated by echocardiography, Evans blue and triphenyltetrazolium chloride staining. Real-time polymerase chain reaction, Western blot, hematoxylin & eosin staining, and immunohistochemistry were utilized to detect the content of mitochondrial DNA, NOD receptor family protein 3 (NLRP3) inflammasome activation, neutrophil recruitment and macrophage infiltration in blood samples and myocardium below the ligation.

Results: We found that EA preconditioning could accelerate the recovery of left ventricle function after MIRI and reduce the myocardial infarction area, thereby protecting the myocardium against MIRI. Furthermore, EA preconditioning was observed to ameliorate mitochondrial impairment, reduce the level of plasma mitochondrial DNA, modulate NLRP3 inflammasome activation, attenuate neutrophil infiltration, and promote the polarization of M1 macrophages towards M2 macrophages in the myocardium after MIRI.

* Corresponding author. Key Laboratory of Acupuncture and Medicine Research of Ministry of Education, Nanjing University of Chinese Medicine, Nanjing, 210023, China.
** Corresponding author. Key Laboratory of Acupuncture and Medicine Research of Ministry of Education, Nanjing University of Chinese Medicine, Nanjing 210023, China.
E-mail addresses: lushengfeng@njucm.edu.cn (S.-F. Lu), 270973@njucm.edu.cn (Y.-H. Gu).
[1] These authors contributed equally to this work.

https://doi.org/10.1016/j.heliyon.2023.e19396
Received 11 December 2022; Received in revised form 11 August 2023; Accepted 21 August 2023
Available online 29 August 2023

Conclusion: EA preconditioning could reduce plasma mtDNA, suppress overactivation of the NLRP3 inflammasome, facilitate the transition from the acute pro-inflammatory phase to the anti-inflammatory reparative phase after MIRI, and ultimately confer cardioprotective benefits.

1. Introduction

Coronary heart disease is the leading cause of mortality among cardiovascular diseases [1]. The restoration of blood flow after coronary artery occlusion is a critical intervention in clinic. Nevertheless, reperfusion may lead to further myocardial injury, specifically myocardial ischemia-reperfusion injury (MIRI). The pathogenesis of MIRI is complex, and a secure and effective treatment for this condition is currently unavailable [2]. How to alleviate MIRI is the focus of current research.

Accumulating evidence has demonstrated the involvement of inflammatory response in the whole process of MIRI and plays a critical role in determining myocardial infarction size and subsequent adverse left ventricular (LV) remodeling [3]. Animal studies have indicated that numerous anti-inflammatory strategies can effectively reduce myocardial infarction size and prevent adverse myocardial remodeling after reperfusion, thereby providing significant myocardial protection [4,5]. However, when these anti-inflammatory strategies were applied in the clinic, most failed to exert cardiac protective effects [6]. It is speculated that the majority of anti-inflammatory strategies concentrate solely on a singular component of the inflammatory response, such as particular cytokines or immune cells, while ignoring the complexity and dynamics of the inflammatory response during MIRI [6]. Therapeutic strategies that focus on the dynamic inflammatory response after myocardial injury may prove more efficacious in the amelioration of damaged myocardium.

The dynamic inflammatory response during MIRI mainly involves two distinct yet overlapping stages, namely the acute pro-inflammatory phase and the anti-inflammatory reparative phase [3]. During the acute pro-inflammatory phase, neutrophils are initially recruited to the injured myocardium to eliminate dead myocardial cells by secreting cytokines and inflammatory factors [7]. The up regulation of pro-inflammatory cytokines and chemokines such as interleukin-1β (IL-1β), induced nitric oxide synthase (iNOS), and chemokine C–C motif ligand 2 (CCL2), serve as markers of the acute pro-inflammatory phase [3]. The anti-inflammatory reparative phase is mainly responsible for the reduction of inflammatory response and fostering the differentiation of fibroblast and angiogenesis, characterized by elevated expression of interleukin-10 (IL-10), transforming growth factor-β (TGF-β) and vascular endothelial growth factor (VEGF) [8]. In addition to neutrophils, macrophages are also crucial in the transition from acute pro-inflammatory to anti-inflammatory reparation [9]. Polarization of two main phenotypes occurs with macrophage activation, namely M1 and M2 macrophages. M1 macrophages are are primarily associated with inflammatory responses, whereas M2 macrophages are capable of regulating vascular remodeling, fibroblast differentiation and collagen production and are crucial for tissue repair [10]. A prompt and systematic transition from the acute pro-inflammatory phase to the anti-inflammatory reparative phase is contribute to alleviating myocardial injury during MIRI.

Acupuncture therapy has been reported to provide myocardial protection. Clinical trials has demonstrated that acupuncture, as an adjunctive therapy for chronic angina pectoris, can significantly reduce the frequency and severity of angina pectoris and maintain a high level of safety [11]. Additionally, acupuncture has been found to possess a notable anti-inflammatory effect, as evidenced by its efficacy in treating inflammatory bowel disease [12] and ulcerative colitis [13]. Ma et al. have revealed that electroacupuncture (EA) modulates the systemic inflammatory response induced by lipopolysaccharide via the autonomic neural pathway, establishing a robust scientific foundation for the use of acupuncture in regulating inflammatory response [14]. Simultaneously, Zhang et al. have reported that EA preconditioning can enhance M2 polarization of macrophages and decrease the infiltration of neutrophils in injured myocardium [15]. Furthermore, our prior investigation demonstrated that EA preconditioning significantly decreased the myocardial infarction size and the level of IL-1β in the myocardium [16]. It is thus clear that EA can promote myocardial protection by regulating inflammation. However, the precise regulatory properties and mechanism of EA on the dynamic inflammatory response in MIRI remains incompletely understood.

In this study, we hypothesized that EA preconditioning might effectively modulate the dynamic inflammatory response occurred during MIRI, ultimately leading to a cardioprotective effect. To investigate this hypothesis, we selected three time points (6h, 24h and 3d) for analysis. Echocardiography, Evans blue and triphenyltetrazolium chloride (TTC) staining were employed to evaluate the cardioprotective effect of EA preconditioning. The mitochondrial DNA, activation of the NOD receptor family protein 3 (NLRP3) inflammasome, infiltration of neutrophils and macrophages were detected to elucidate the dynamic inflammatory response and associated mechanisms of EA in MIRI rats.

2. Materials and methods

2.1. Experimental animals

Male Sprague Dawley rats (2 months old, 250 ± 20 g) were purchased from Charles River Laboratories (SCXK 2016-0006). For one week before the experiment, the rats were acclimatized to a 12-h light/dark cycle in a controlled environment with a temperature of approximately 25 °C and relative humidity of 50%. They had free access to standard mouse chow and tap water. This study was conducted in accordance with the National Institutes of Health's Guide for the Care and Use of Laboratory Animals and was approved by the Animal Ethics Committee of Nanjing University of Chinese Medicine Laboratory Animal Center (Permit number: 202004A009).

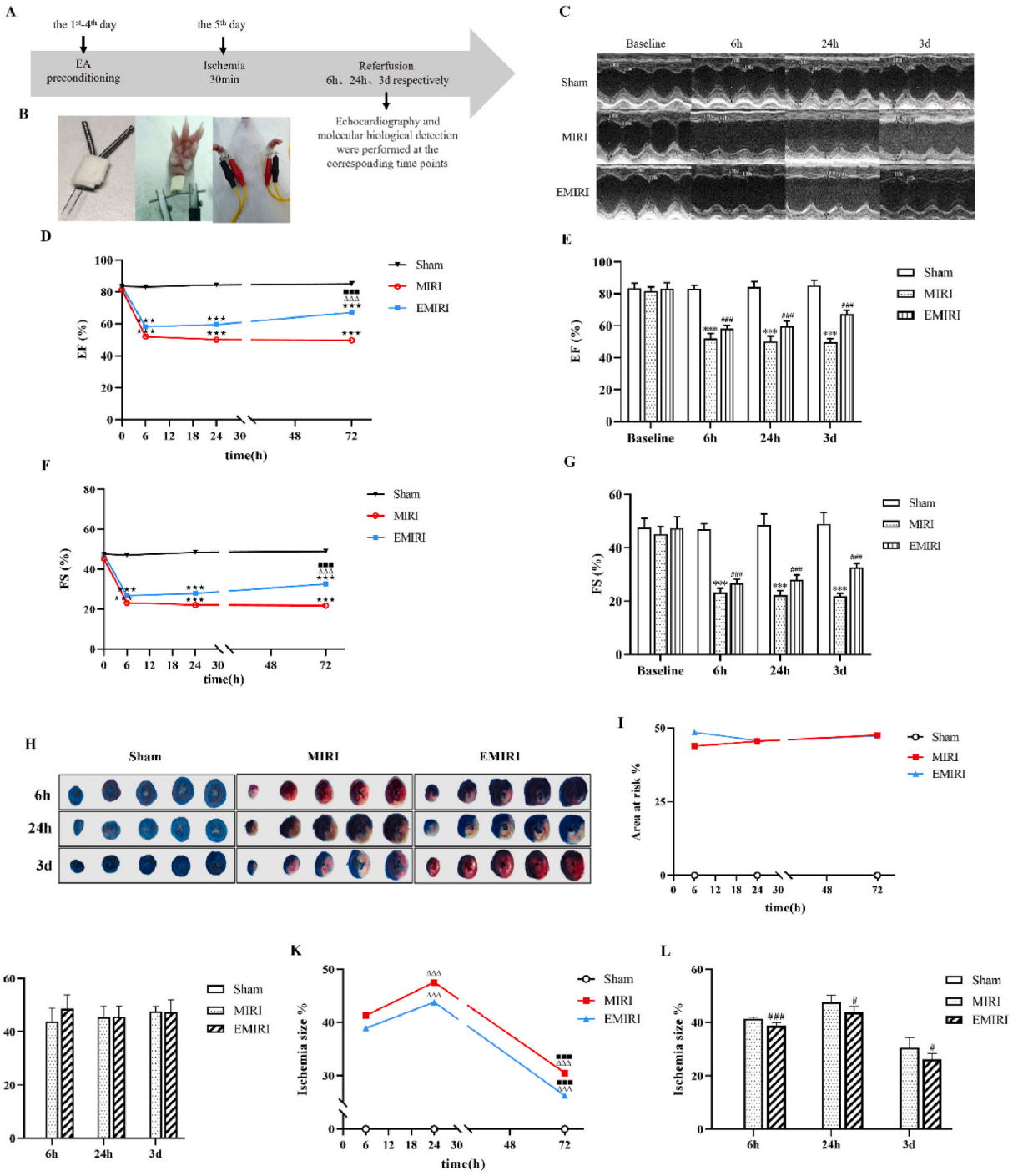

Fig. 1. Cardioprotection of EA preconditioning against MIRI at different time points (n = 5–6 in each group). (A) The experimental protocol used to explore the cardioprotection of EA preconditioning in a rat model of MIRI. (B) Schematic diagram of EA operation. (C) Representative M-mode of echocardiographic recordings of each group. (D) Comparison of EF levels at different time points in each group. (E) Intergroup comparison of EF levels in rats at different time points. (F) Comparison of FS levels at different time points in each group. (G) Intergroup comparison of FS levels in rats at different time points. (H) Representative Evans blue/TTC staining of the hearts. (I) Comparison of the area at risk% at different time points in each group. (G) Intergroup comparison of the area at risk% in rats at different time points. (K) Comparison of ischemia size% at different time points in each group. (L) Intergroup comparison of ischemia size% in rats at different time points. $^{***}p < 0.001$ vs Baseline; $^{\triangle\triangle\triangle}p < 0.001$ vs 6h; $^{\blacksquare\blacksquare\blacksquare}p < 0.001$ vs 24h; $^{***}p < 0.001$ vs Sham; $^{\#}p < 0.05$ vs MIRI, $^{\#\#\#}p < 0.001$ vs MIRI. Sham: sham operation group; MIRI: MIRI model group; EMIRI: EA preconditioning plus MIRI model group. Baseline: before MIRI; 6h: 6h after reperfusion; 24h: 24h after reperfusion; 3d: 3d after reperfusion.

2.2. Animal grouping and experimental design

After one week of acclimatization, the rats were randomly divided into three groups: (i) In the sham operation group (Sham), they underwent a sham operation consisting of left thoracotomy but without the ligation of the left anterior descending (LAD) coronary artery. (ii) In the MIRI model group (MIRI), MIRI was induced by ligating LAD for 30 min, followed by reperfusion. (iii) In the EA preconditioning plus MIRI model group (EMIRI), the rats received four days of EA at bilateral Neiguan point (PC6) before MIRI. Corresponding detection and sampling were performed at 6h, 24h and 3d after reperfusion in each group. The experimental protocols were shown in Fig. 1A.

2.3. MIRI model establishment and EA preconditioning

The rats were anesthetized with 5% isoflurane (R510-22, RWD) plus purity oxygen, and then the concentration of isoflurane was maintained at 1–2%. Rats were then placed supine on a temperature-controlled experimental board set at 37 ± 3 °C and intubated with a small animal ventilator (R407, RWD) set at a respiratory rate of 60–70 breaths per minute. After disinfecting the surgical area, the left chest was opened to expose the heart at the 3rd intercostal space. The pericardium was separated, the heart was exteriorized, and the LAD was quickly ligated with the 6.0 prolene suture, approximately 2 mm in width and depth, to induce myocardial ischemia. The paler color below the ligation area seemed to be a successful occlusion of LAD. After 30 min of ischemia, the suture was removed to allow reperfusion.

According to the previous study [17], rats in the EMIRI group received consecutive 4 days of EA preconditioning on PC6 before MIRI induction (Fig. 1B). EA intervention parameters are the same as previously described [18,19]: bipolar acupuncture needles were inserted to a depth of 2–3 mm and approximately 3 mm proximal to the palm crease above the median nerve. After insertion, the needles were connected to Han's Acupoint Nerve Stimulator (WQ1002F, Han Acuten) and stimulated with an intensity of 2 mA and frequency of 2/100 Hz for 20 min per day.

2.4. Echocardiography recording

LV function was assessed by transthoracic M-mode echocardiography at the corresponding time point before and after MIRI. The measurement protocol is detailly described in our previous study [20]. The ejection fraction (EF) and fractional shortening (FS) were calculated according to the following formula: FS= (left ventricular internal diameter at end-diastole (LVIDd)- left ventricular internal diameter at end-systole (LVIDs))/LVIDd × 100%; EF = (left ventricular end-diastolic volume (LV Vol; d) – left ventricular end-systolic volume (LV Vol; s))/(LV Vol; d) × 100%.

2.5. Assessment of myocardial infarction area

Evans Blue and TTC staining were used to visualize the area of myocardial infarction in MIRI and EMIRI groups. Specific operations are as follows: the aorta was clipped after re-ligating the LAD, and 0.6 ml of 2% Evans blue (E2129, Sigma) was injected into the left ventricle from the aorta. The hearts were then quickly harvested after blue stained and frozen at −80 °C. The frozen myocardial tissue below the ligation site was sliced into five sections of approximately 1–2 mm each and placed in 2% TTC (T8170, Sigma) for 10 min at 37 °C in a dark incubator. The stained heart slices were fixed in 4% paraformaldehyde, photographed and analyzed using the image analysis software Image-ProPlus. There were three main zones in the stained myocardial tissue: the blue areas were normal tissue with no infarction, the non-blue area was myocardial tissue at risk (area at risk, the ligated LAD was responsible for the blood supply to this part of the myocardium), including the infarct tissue appeared white and the viable myocardium after ischemia appeared red. The severity of myocardial infarction was assessed using the following formulae: percentage of area at risk = areas at risk/total myocardial areas × 100%; percentage of ischemia area = infract areas/areas at risk × 100%.

2.6. Western blot (WB) analysis

The myocardial tissues below the ligation were collected and stored in the refrigerator at −80 °C. Frozen myocardial tissues were homogenized in radioimmunoprecipitation assay (RIPA) buffer with a 100 mg: 1 mL ratio, then centrifuged at 12000 rpm for 10 min at 4 °C. Bicinchoninic acid (BCA) protein assay (23227, Thermo Fisher) was performed using the supernatants to determine protein concentration. The proteins were then loaded and separated on SDS-polyacrylamide gel electrophoresis (SDS-PAGE), then transferred to the polyvinylidene difluoride (PVDF) membrane. Following this, the membranes were blocked for 2 h and then incubated with primary antibodies for cytochrome *c* (cyto C, 1:1000, 10993-1-AP, Proteintech), NLRP3 (1:1000, bs-10021R, Bioss), ASC (1:1000, bs-6741R, Bioss), caspase 1 (1:1000, BS90183, Bioworlde), pro-caspase 1 (1:1000, ab179515, Abcam) and TLR 9 (1:1000, DF2970, Affinity Biosciences) overnight at 4 °C. After washing three times for 10 min each, the membranes were incubated with secondary antibodies (1:5000, SA00001-1 or SA00001-2, Proteintech) for 2 h. Anti-β-actin (1:4000, 66009-1-Ig, Proteintech) and COX IV (1:4000, 11242-1-AP, Proteintech) were the loading control protein. The bands were imaged and analyzed using the Bio-Imaging system. Tissue mitochondria isolation kit (C3606, Beyotime) was used to extract myocardial mitochondria for WB detection of mit-cyto C.

2.7. Quantitative real-time polymerase chain reaction (RT-qPCR)

RT-qPCR was used to measure the mRNA expressions of mitochondrial deoxyribonucleic acid (mtDNA) and myeloperoxidase (MPO). After extracting total RNAs in myocardial tissues with TRIzol (15596018, Thermo Scientific), cDNA was synthesized by reverse transcription and amplified by a real-time fluorescence quantitative PCR system (IQ5TM, Bio-Rad). Amplification was carried out by denaturing at 94 °C for 30 s, annealing at 55 °C for 45 s, and extending at 72 °C for 30 s for 40 cycles. The primer sequences are listed in Table 1. GAPDH was used as an internal control. Each sample was analyzed three times, and the relative expressions of genes were determined using the $2^{-\Delta\Delta CT}$ method.

2.8. Hematoxylin & eosin staining

Hematoxylin & eosin staining (H&E) staining was used for the evaluation of inflammatory cell infiltration. The ventricular tissues fixed in 4% paraformaldehyde were dehydrated, paraffin-embedded, and sliced into 4 μm thick sections. The sections were then stained with hematoxylin and eosin. After H&E staining, the sections were dehydrated and observed under an optical microscope. Myocarditis severity was scored on H&E-stained sections using grades from 0 to 4: 0, no inflammation; 1, <25% of the heart section involved; 2, 25–50%; 3, 50–75%; and 4, >75% [21].

2.9. Immunohistochemistry analysis

Myocardial tissues below the ligation line were collected and fixed with 4% paraformaldehyde to assess IL-1β, cluster of differentiation 86 (CD86), TGF-β and cluster of differentiation 206 (CD206) by immunohistochemistry (IHC). The fixed myocardium was dehydrated, paraffin-embedded, sectioning, paraffin sectioning dewaxed to water, antigen reparation, endogenous peroxidase blocking, serum blocking, primary antibody overnight, secondary antibody overnight, DAB staining, nuclear restaining, sectioning dehydrated and sealed, and microphotography. The dilution ratio of the primary antibody was IL-1β (1:800, GB11113, Servicebio), CD86 (1:400, GB13585, Servicebio), TGF-β (1:500, GB11179, Servicebio), CD206 (1:10000, GB13438, Servicebio). The dilution ratio of the second antibody (GB23303, Servicebio) was 1:200. Servicebio image analysis system was used to read collected tissue image automatically. The number of weak, medium, vital positive cells and the total cell number were calculated. Evaluation criteria of expression intensity: negative, no staining; Weak positive, light yellow; Moderate positive, light tan; Strong positive: tan. H score = $\sum$ (pi × i) = (percentage of weak intensity cells × 1)+(percentage of moderate intensity Cells × 2)+(percentage of strong intensity cells × 3), pi was the ratio of positive cells, i was color intensity. The h-score is between 0 and 300, and the larger the data, the stronger the comprehensive positive intensity [22].

2.10. Statistical analysis

Statistical analyses were completed using IBM SPSS 25.0. Data were checked for normality by applying the Shapiro-Wilk test and were presented as mean ± standard deviation when normally distributed, while a boxplot showing all points was used when the data did not meet the normal distribution. For EF and FS, the generalized linear model was used to merge and pairwise compare the data at each time point, and holm-Bonferroni was used to correct multiple comparisons. For other data, if the data were normally distributed, groups were compared by one-way analysis of variance (ANOVA), followed by Fisher's LSD method (equal variances assumed) or Dunnett's T3 method (equal variances not assumed). Kruskal Wallis was used to compare the difference between groups if the data did not follow the normal distribution assumption. A p value < 0.05 was considered statistically significant.

3. Results

3.1. EA preconditioning alleviated myocardial injury after MIRI

The echocardiography and Evans Blue and TTC staining were used to evaluate the myocardial protection of EA preconditioning. The motion of the anterior wall of the left ventricle was attenuated after reperfusion in both MIRI and EMIRI groups (Fig. 1C). In the MIRI group, the anterior wall movement of the LV was decreased at 6h and 24h after reperfusion, but slightly improved at 3d after reperfusion (Fig. 1C); The EF and FS were significantly reduced at 6h, 24h and 3d after reperfusion compared with the baseline, but no statistical difference was observed between the three time points (Fig. 1 D and F). The anterior wall movement of the left ventricle in the EMIRI group was slightly improved at 24h compared with 6h after reperfusion, and improved at 3d markedly (Fig. 1C); The EF and FS were significantly decreased at 6h, 24h and 3d after reperfusion compared with the baseline. And interestingly, the EF and FS were

Table 1
Sequence of genes.

Gene Name	Forward:	Reverse:
mtDNA	AACGCAGCTTAACATTCCGC	CTGGTTGGCCTCCGATTCAT
MPO	GGGATACAATGCCTGGAGACG	TTGTTGGGCGTGCCATACTG
GAPDH	CTGGAGAAACCTGCCAAGTATG	GGTGGAAGAATGGGAGTTGCT

increased at 3d compared with 6h and 24h after reperfusion (Fig. 1 D and F). At each time point after reperfusion, the EMIRI group had better left ventricular anterior wall movement and increased EF and FS than the MIRI group (Fig. 1C, E and G).

Evans Blue and TTC staining was operated to reflect the myocardial infarct size (Fig. 1H). There was no statistical difference between MIRI and EMIRI groups in the area at risk % at any time (Fig. 1 I and J). Since the area at risk % reflects the myocardial region which the ligated LAD provides blood to, no difference between these two groups suggested that our model of MIRI was successful and stable. In the MIRI group, compared with 6h after reperfusion, the ischemia size % increased at 24h; Compared with 24h after

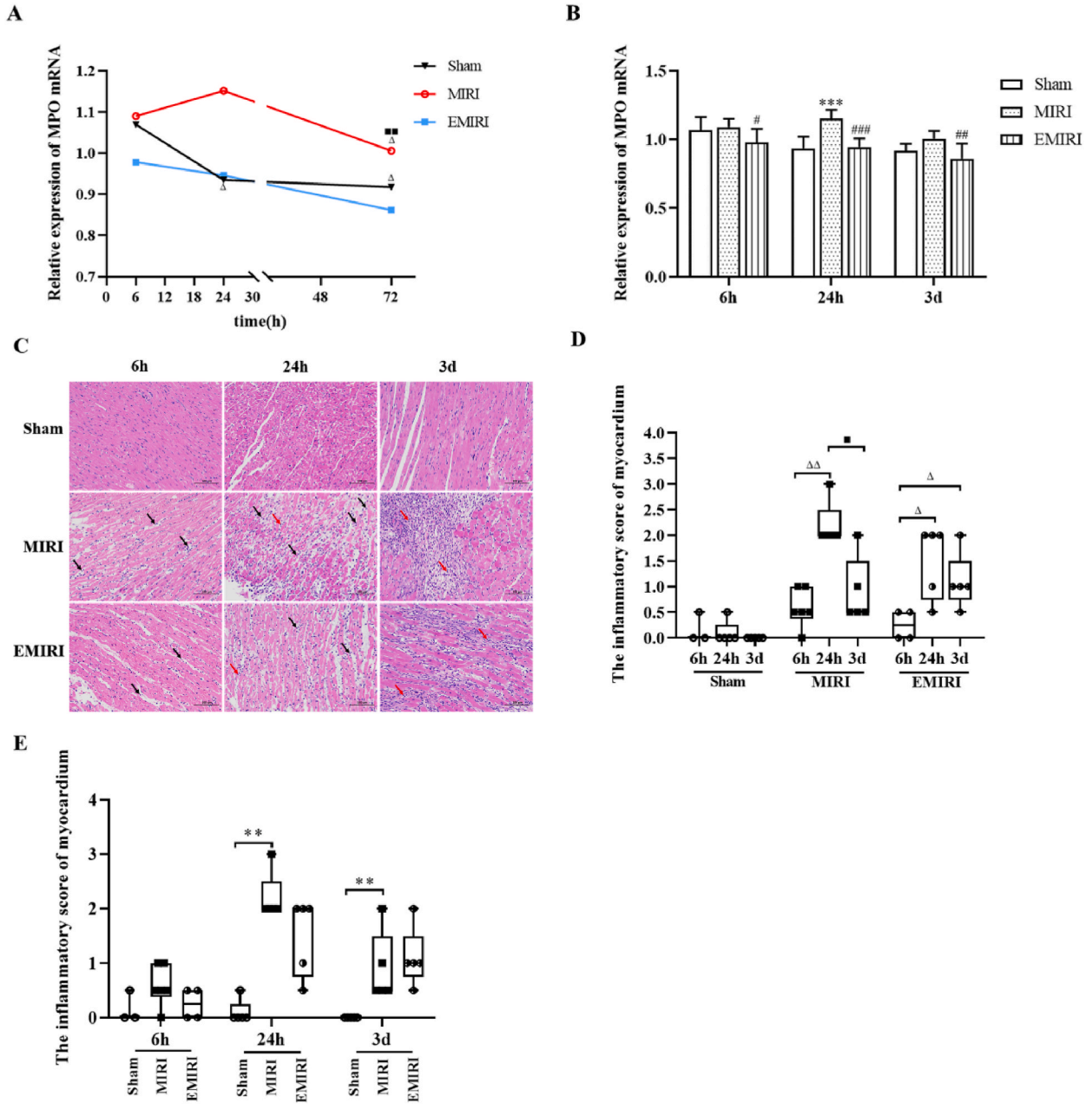

Fig. 2. Effect of EA preconditioning on neutrophils infiltration after MIRI (n = 3–6 each group). (A)Comparison of relative expression of MPO at different time points in each group detected by RT-qPCR. (B) Intergroup comparison of relative expression of MPO in rats at different time points detected by RT-qPCR. (C) Representative HE-stained myocardial sections. Black arrows were used to mark neutrophils, and red arrows were used to mark monocytes. (D) Comparison of the inflammatory score of myocardium at different time points in each group. (E) Intergroup comparison of the inflammatory score of myocardium at different time points. $^{\triangle}p < 0.05$ vs 6h, $^{\triangle\triangle}p < 0.01$ vs 6h; $^{\blacksquare}p < 0.05$ vs 24h, $^{\blacksquare\blacksquare}p < 0.01$ vs 24h; $^{**}p < 0.01$ vs Sham, $^{***}p < 0.001$ vs Sham; $^{\#}p < 0.05$ vs MIRI, $^{\#\#}p < 0.01$ vs MIRI, $^{\#\#\#}p < 0.001$ vs MIRI. Sham: sham operation group; MIRI: MIRI model group; EMIRI: EA preconditioning plus MIRI model group. 6h: 6h after reperfusion; 24h: 24h after reperfusion; 3d: 3d after reperfusion.

reperfusion, the ischemia size % was significantly decreased at 3d reperfusion (Fig. 1K). The change of ischemia size % in EMIRI showed the same trend as MIRI (Fig. 1K). Compared with the MIRI group, the ischemia size % decreased at all time points in the EMIRI group (Fig. 1L).

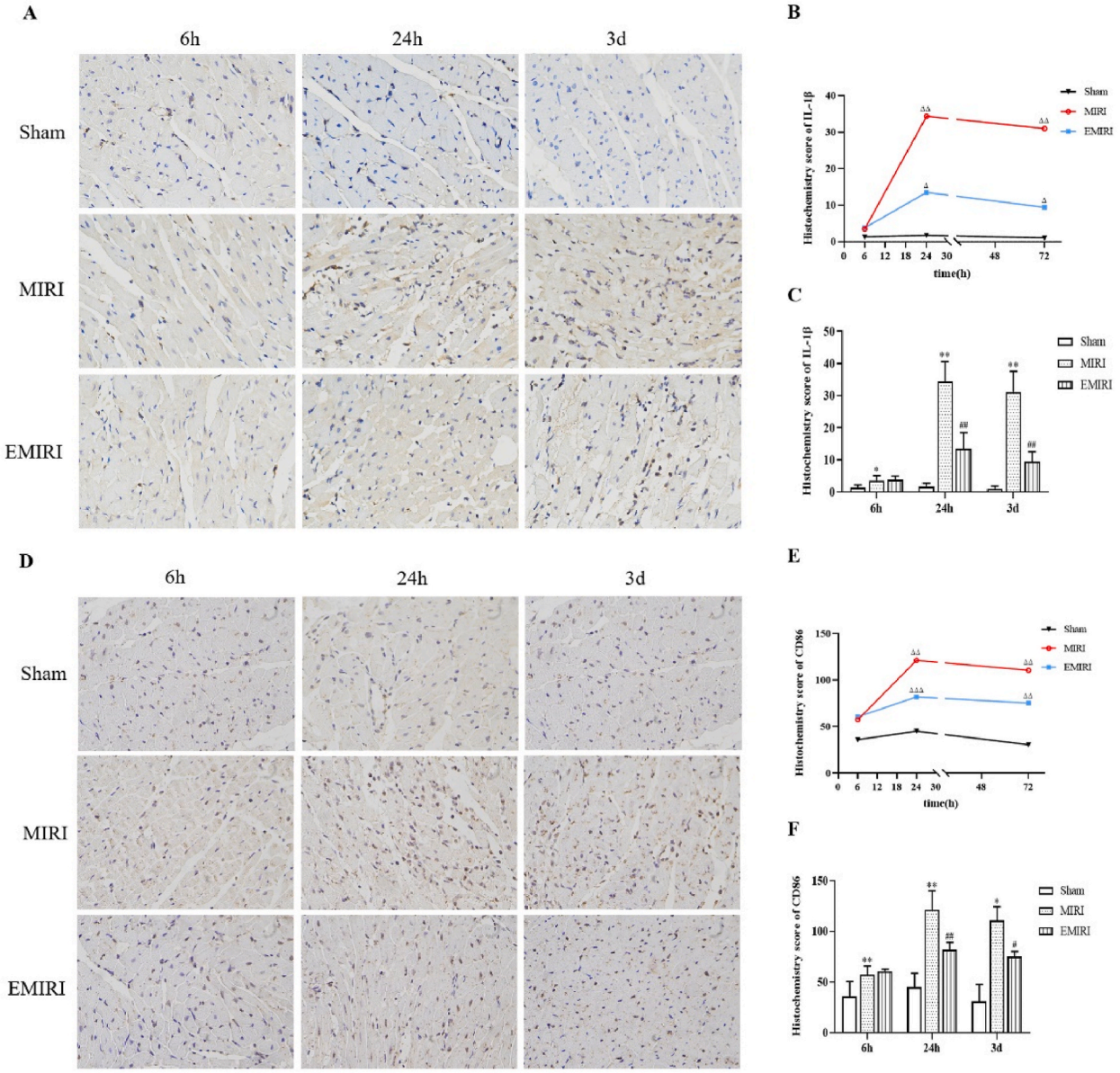

Fig. 3. Effect of EA preconditioning on the polarization of macrophages (n = 3–6 each group). (A) Representative IHC staining of IL-1β. (B) Comparison of relative expression of IL-1β at different time points in each group. (C) Intergroup comparison of relative expression of IL-1β in rats at different time points. (D) Representative IHC staining of CD86. (E) Comparison of relative expression of CD86 at different time points in each group. (F) Intergroup comparison of relative expression of CD86 in rats at different time points. (G) Representative IHC staining of TGF-β. (H) Comparison of relative expression of TGF-β at different time points in each group. (I) Intergroup comparison of relative expression of TGF-β in rats at different time points. (J) Representative IHC staining of CD206. (K) Comparison of relative expression of CD206 at different time points in each group. (L) Intergroup comparison of relative expression of CD206 in rats at different time points. Magnification: × 400. $^{\triangle}p < 0.05$ vs 6h, $^{\triangle\triangle}p < 0.01$ vs 6h, $^{\triangle\triangle\triangle}p < 0.001$ vs 6h; $^{\blacksquare\blacksquare}p < 0.01$ vs 24h, $^{\blacksquare\blacksquare\blacksquare}p < 0.001$ vs 24h; $^{*}p < 0.05$ vs Sham, $^{**}p < 0.01$ vs Sham, $^{***}p < 0.001$ vs Sham; $^{\#}p < 0.05$ vs MIRI, $^{\#\#}p < 0.01$ vs MIRI, $^{\#\#\#}p < 0.001$ vs MIRI. Sham: sham operation group; MIRI: MIRI model group; EMIRI: EA preconditioning plus MIRI model group. 6h: 6h after reperfusion; 24h: 24h after reperfusion; 3d: 3d after reperfusion.

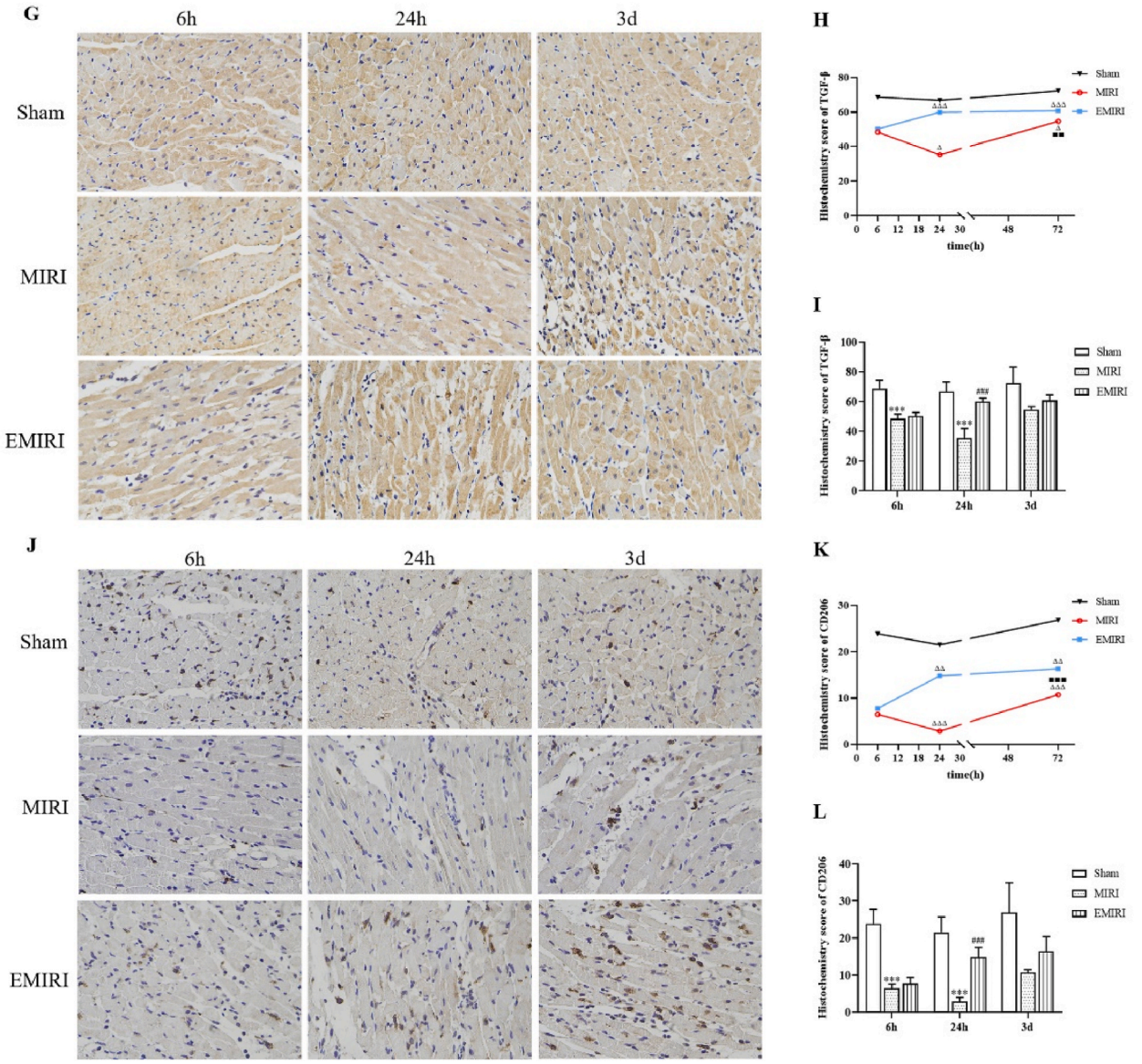

Fig. 3. (*continued*).

3.2. EA preconditioning alleviated neutrophils infiltration after MIRI

Myeloperoxidase (MPO) is mainly expressed in the neutrophil. Therefore, the infiltration degree of neutrophils in myocardial tissue can be determined by the level of MPO [23]. We found that, in the MIRI group, the level of MPO increased at 24h compared with 6h after reperfusion and decreased at 3d compared with 24h after reperfusion (Fig. 2 A). In the EMIRI group, the expression of MPO gradually reduced over time, but there was no statistical difference among the three time points after reperfusion (Fig. 2 A). Compared with the MIRI group, the expression of MPO decreased at all time points in the EMIRI group (Fig. 2 B). We also scored the myocarditis severity on H&E-stained sections (Fig. 2C), the results showed that, in the MIRI group, the inflammatory score increased at 24h compared with 6h after reperfusion, and decreased at 3d compared with 24h after reperfusion (Fig. 2 D). In the EMIRI group, the inflammatory score increased at 24h and 3d compared with 6h after reperfusion (Fig. 2 D). Compared with the MIRI group, the inflammatory score decreased at 6h and 24h in the EMIRI group, but there was no statistical difference (Fig. 2 E).

3.3. EA preconditioning contributed to the transformation of M1 macrophages to M2 macrophages after MIRI

IHC was used to detect the expression of M1 and M2 macrophages in the myocardium. We detected IL-1β (Fig. 3 A) and CD86 (Fig. 3 D) which were the markers of M1 macrophage, and TGF-β (Fig. 3 G) and CD 206 (Fig. 3 J) which were the markers of M2 macrophage.

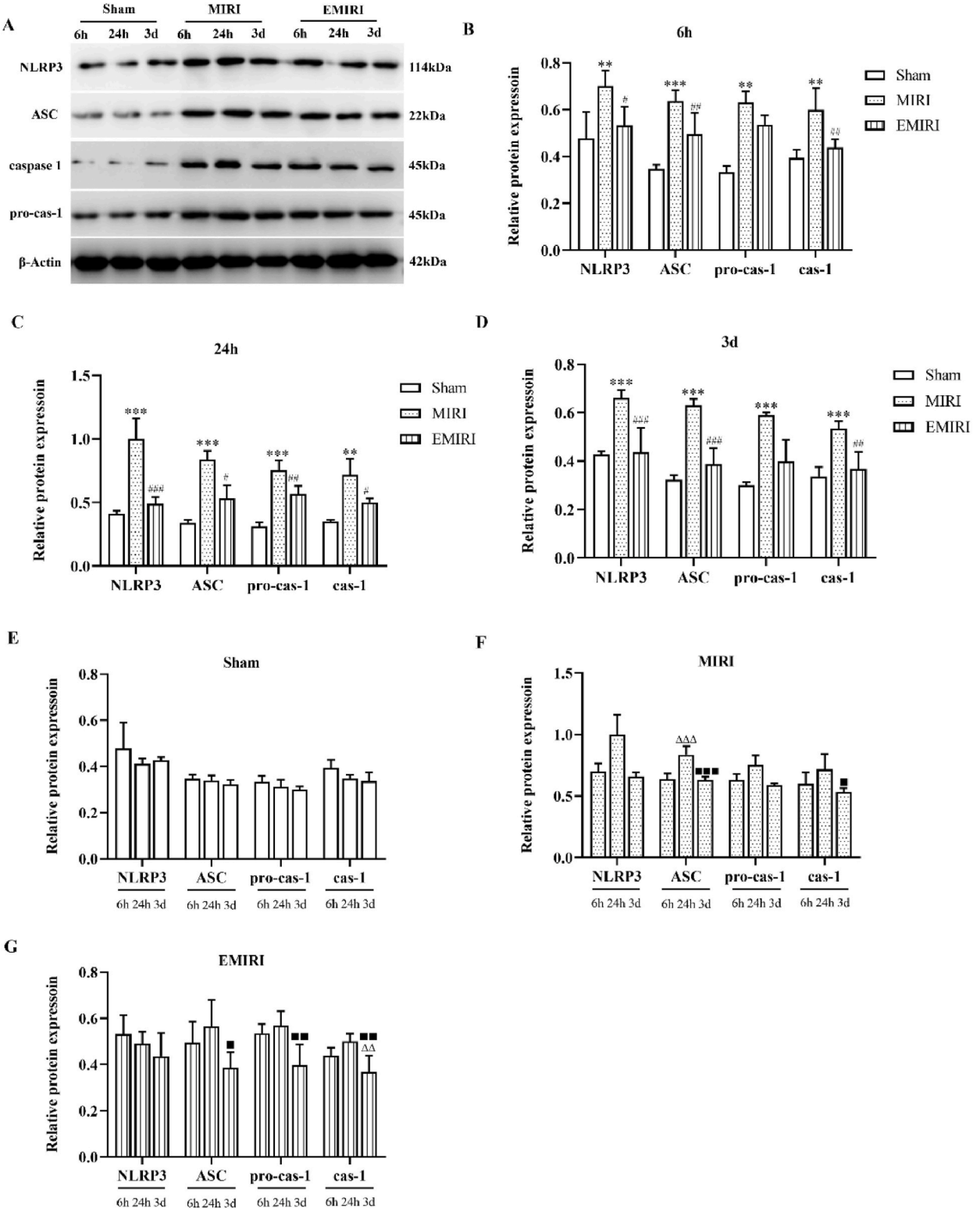

(caption on next page)

Fig. 4. MIRI-induced NLRP3 inflammasome activation was regulated by EA preconditioning (n = 3–5 in each group). (A) Expression of NLRP3 inflammasome and TLR9 detected by WB. (B) The relative expression of NLRP3 inflammasome in each group at 6h after reperfusion. (C) The relative expression of NLRP3 inflammasome in each group at 24h after reperfusion. (D) The relative expression of NLRP3 inflammasome in each group at 3d after reperfusion. (E) The relative expression of NLRP3 inflammasome at different time points in the Sham group. (F) The relative expression of NLRP3 inflammasome at different time points in the MIRI group. (G) The relative expression of NLRP3 inflammasome at different time points in the EMIRI group. $^{\triangle\triangle}p < 0.01$ vs 6h, $^{\triangle\triangle\triangle}p < 0.001$ vs 6h; $^{\blacksquare}p < 0.05$ vs 24h, $^{\blacksquare\blacksquare}p < 0.01$ vs 24h, $^{\blacksquare\blacksquare\blacksquare}p < 0.001$ vs 24h; $^{**}p < 0.01$ vs Sham, $^{***}p < 0.001$ vs Sham; $^{\#}p < 0.05$ vs MIRI, $^{\#\#}p < 0.01$ vs MIRI, $^{\#\#\#}p < 0.001$ vs MIRI. Sham: sham operation group; MIRI: MIRI model group; EMIRI: EA preconditioning plus MIRI model group. 6h: 6h after reperfusion; 24h: 24h after reperfusion; 3d: 3d after reperfusion.

In the MIRI group, the expression of IL-1β and CD86 increased, while TGF-β and CD 206 decreased at 24h compared with 6h after reperfusion; The expression of TGF-β and CD 206 increased, but there was no statistical difference in the expression of IL-1β and CD86 at 3d compared with 24h after reperfusion (Fig. 3 B, E, H, K). In the EMIRI group, the expression of IL-1β, CD86, TGF-β and CD 206 both increased at 24h compared with 6h after reperfusion; The expression of IL-1β and CD86 decreased, while there was no statistical difference in the expression of TGF-β and CD 206 at 3d compared with 24h after reperfusion (Fig. 3 B, E, H, K). At 6h after reperfusion, there was no statistical difference in the expression of the four markers in the MIRI and EMIRI group; at 24h after reperfusion, compared with the MIRI group, the expression of IL-1β and CD86 decreased, and TGF-β and CD 206 increased in EMIRI group; at 3d after reperfusion, the expression of IL-1β and CD86 decreased, and there was no statistical difference in the expression of TGF-β and CD 206 in EMIRI group compared with MIRI group (Fig. 3C, F, I, L).

3.4. EA preconditioning regulated the activation of NLRP3 inflammasome in the myocardium of MIRI rat

The activation of NLRP3 inflammasome in the myocardium of rats was detected by WB (Fig. 4 A). Briefly, in the Sham group, the activation of NLRP3 inflammasome showed no significant changes among the three time points (Fig. 4 E). In the MIRI group, there was no statistical difference in the expression of NLRP3 and pro-caspase 1 among the three time points; The expression of the apoptosis-related speckle-like protein (ASC) increased at 24h compared with 6h after reperfusion; The expression of ASC and caspase 1 decreased at 3d compared with 24h after reperfusion (Fig. 4 F). In the EMIRI group, the expression of ASC, pro-caspase 1 and caspase 1 decreased at 3d compared with 24h after reperfusion (Fig. 4 G). At each time point after reperfusion, the expression of NLRP3, ASC, pro-caspase 1 and caspase 1 both decreased in the EMIRI group compared with the MIRI group (Fig. 4B–D).

3.5. EA preconditioning ameliorated plasma mtDNA in the myocardium of MIRI rat

The level of cytosolic cytochrome C (cyt-cyto C), mitochondrial cytochrome C (mit-cyto C) and free mtDNA were detected to evaluate mitochondrial integrity in myocardial tissue (Fig. 5 A and B). We found that, in the MIRI group, compared with 6h after reperfusion, the expression of mit-cyto C decreased, cyt-cyto C and mtDNA increased at 24h; While mit-cyto C increased, cyt-cyto C and mtDNA decreased at 3d compared with 24h after reperfusion (Fig. 5C, E and G). The change of mit-cyto C, cyt-cyto C and mtDNA in EMIRI showed the same trend as MIRI at each time point after reperfusion (Fig. 5C, E and G). At 6h and 24h reperfusion, compared with the MIRI group, the mit-cyto C increased, while the cyt-cyto C and mtDNA decreased in the EMIRI group (Fig. 5 D, F and H); At 3d after reperfusion, the mit-cyto C increased and the cyt-cyto C decreased compared with MIRI group, while there was no difference of mtDNA between MIRI and EMIRI groups (Fig. 5 D, F and H).

It has been reported that free mtDNA can be recognized by TLR9 and trigger NLRP3 inflammasome activation [24]. In the MIRI group, the expression of TLR9 increased at 24h compared with 6h after reperfusion and decreased at 3d compared with 24h after reperfusion (Fig. 5 I). In the EMIRI group, the expression of TLR9 gradually reduced over time (Fig. 5 I). At 6h after reperfusion, there was no difference between MIRI and EMIRI groups; At 24h and 3d, the expression of TLR9 decreased in the EMIRI group compared with the MIRI group (Fig. 5 J).

4. Discussion

Previous researches have reported that EA preconditioning can mitigate ventricular arrhythmia [18], reduce infarct size and enhance left ventricle function [15] after MIRI. In this study, we evaluate the myocardial protective effect of EA preconditioning by echocardiography and Evans Blue-TTC staining. Our findings reveal no significant variation in the area at risk ratio between the MIRI and EMIRI groups, indicating the stability and success of our MIRI model. EA preconditioning effectively reversed the reduced left ventricle function at three time points and decreased the ratio of infarct size except 6h after reperfusion. These findings provide further evidence that EA preconditioning can protect the myocardium against MIRI. Additionally, the observed increase and subsequent decrease in in the ratio of infarct size in the MIRI group suggested the occurrence of self-regulation in the infarcted myocardium, which is consistent with our previous study [19,20]. The MIRI group exhibited a decline in left ventricle function, with no difference observed at three time points after reperfusion. In contrast, the EMIRI group exhibited a reduction in left ventricle function at 6h and 24h after reperfusion, followed by an improvement at 3d after reperfusion. These findings suggested that EA preconditioning could speed up cardiac repair after MIRI to a certain degree, thereby revealing a novel protective phenomenon.

Distinct inflammatory and immune cells participate in myocardial reparation at different stages after myocardial injury. During the acute pro-inflammatory phase, neutrophils and subsequently recruited M1 macrophages express IL-1β and TNF-α, generate proteolytic enzymes, and secrete matrix metalloproteinases (MMPs) to degrade the extracellular matrix [9]. In the anti-inflammatory reparative

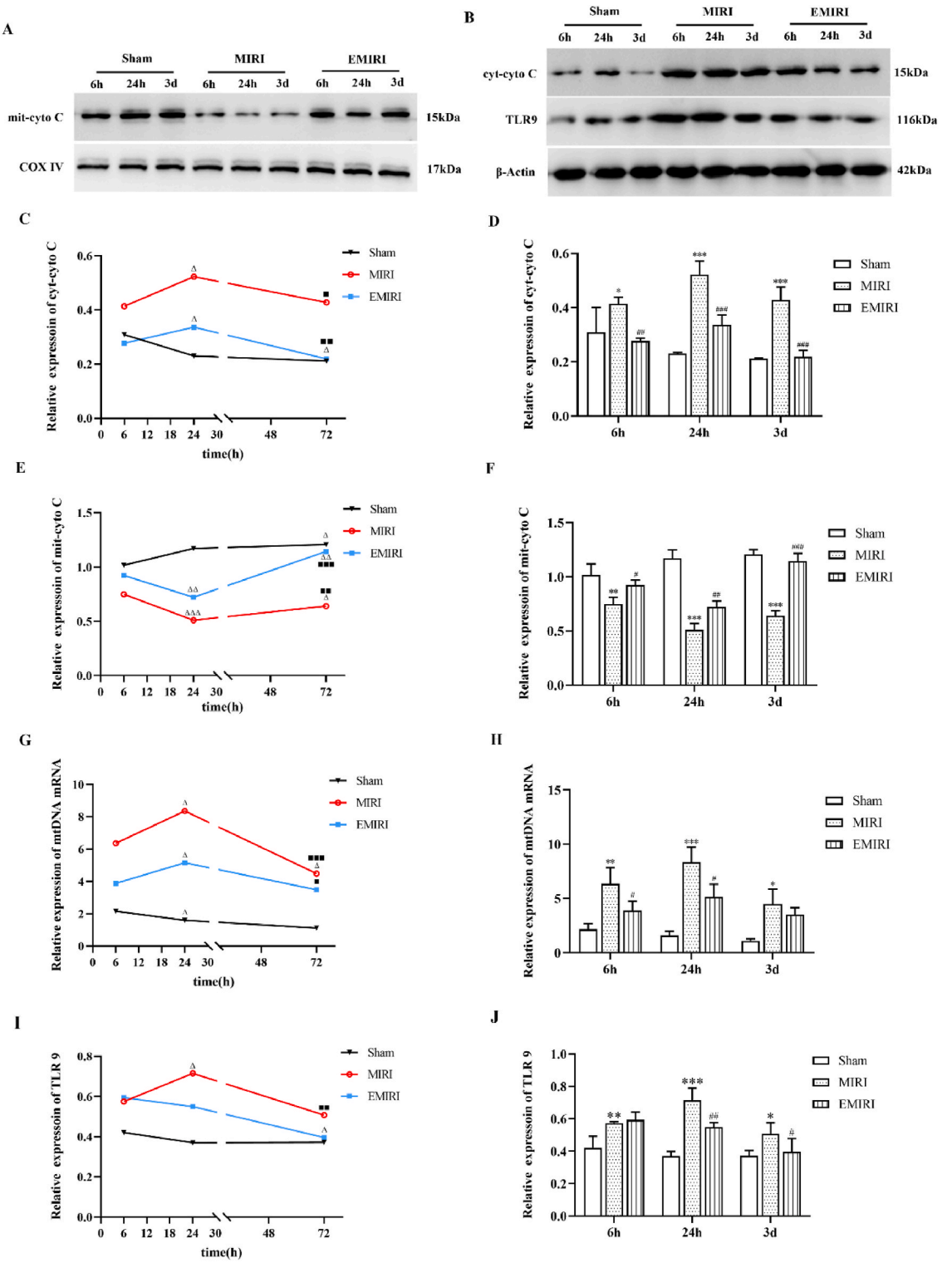

Fig. 5. MIRI-induced plasma mtDNA was attenuated by EA preconditioning (n = 3–6 in each group). (A) Expression of mit-cyto C detected by WB. (B) Expression of cyt-cyto C detected by WB. (C) Comparison of relative expression of cyt-cyto C at different time points in each group. (D) Intergroup comparison of relative expression of cyt-cyto C in rats at different time points. (E) Comparison of relative expression of mit-cyto C at different time points in each group. (F) Intergroup comparison of relative expression of mit-cyto C in rats at different time points. (G) Comparison of relative expression of mtDNA at different time points in each group detected by RT-qPCR. (H) Intergroup comparison of relative expression of mtDNA in rats at different time points detected by RT-qPCR. (I) Comparison of relative expression of TLR9 at different time points in each group. (J)

Intergroup comparison of relative expression of TLR9 in rats at different time points. $^{\triangle}p < 0.05$ vs 6h, $^{\triangle\triangle}p < 0.01$ vs 6h, $^{\triangle\triangle\triangle}p < 0.001$ vs 6h; $^{\blacksquare}p < 0.05$ vs 24h, $^{\blacksquare\blacksquare}p < 0.01$ vs 24h, $^{\blacksquare\blacksquare\blacksquare}p < 0.001$ vs 24h; $^{*}p < 0.05$ vs Sham, $^{**}p < 0.01$ vs Sham, $^{***}p < 0.001$ vs Sham; $^{\#}p < 0.05$ vs MIRI, $^{\#\#}p < 0.01$ vs MIRI, $^{\#\#\#}p < 0.001$ vs MIRI. Sham: sham operation group; MIRI: MIRI model group; EMIRI: EA preconditioning plus MIRI model group. 6h: 6h after reperfusion; 24h: 24h after reperfusion; 3d: 3d after reperfusion.

phase, M2 macrophage, regulatory T cells (Treg) and other immune cells are recruited to the damaged myocardium, which are essential for the remodeling of the infarcted myocardium and the restoration of cardiac function. Rusinkevich V et al. have reported that neutrophil infiltration in the myocardial infarction area reaches its peak one day after reperfusion, while macrophage infiltration peaks at day three after reperfusion, with the primary phenotype being M2 macrophages that maintain a high expression level thereafter [25]. Cristine J et al. reported a significant increase in the infiltration of neutrophils and M1 macrophages, and a decrease in the infiltration of M2 macrophages in the infracted myocardium at 24h after reperfusion. However, at day 3 after reperfusion, the infiltration of neutrophils decreased while the infiltration of M1 and M2 macrophages increased [26]. Another study revealed a progressive enlargement of the myocardial infarction region, with the most significant expansion occurring at 24 h following reperfusion [27]. Our study revealed that in the MIRI group, the infiltration of both neutrophils and M1 macrophages increased, whereas the infiltration of M2 macrophages decreased at 24h of reperfusion. As time progressed, the neutrophil infiltration decreased, and M2 macrophage infiltration increased. It was suggested that the myocardial reparation in the study was in the acute pro-inflammatory phase at 24h reperfusion and gradually entered to the anti-inflammatory reparative phase within 24h-3d after reperfusion, which was consistent with the previous reports [25,26]. The expression of MPO in the EMIRI group was observed to be lower than that in the MIRI group at all time points after reperfusion, suggesting that EA preconditioning might inhibit neutrophil infiltration after MIRI. Additionally, in the EMIRI group, the recruitment of M1 and M2 macrophages was significantly increased at 24h compared with 6h after reperfusion, and there was no significant difference in the expression of markers between 24h and 3d after reperfusion. Through a comprehensive analysis of the infiltration of neutrophils and macrophages, it was hypothesized that the transition from the acute pro-inflammatory phase to the anti-inflammatory reparative phase occurred within a timeframe of 6h–24h after reperfusion in the EMIRI group. We considered that EA preconditioning could accelerate the polarization of M2 macrophages, and facilitate the transition from the acute pro-inflammatory phase to the anti-inflammatory reparative phase after MIRI. Zhang et al. have reported that EA preconditioning can promotes M2 polarization of macrophages and reduces the recruitment of neutrophils in damaged myocardium, thereby decreasing the infarct size and improves the cardiac function [15], which corroborate the findings of our investigation.

The NLRP3 inflammasome, which consists NLRP3, apoptosis-associated speck-like protein ASC and pro-caspase-1, is considered the most widely studied inflammasome [28]. Activation of NLRP3 inflammasome can lead to increased inflammation, resulting in cardiac dysfunction and remodeling [29]. Oridonin, a NLRP3 inflammasome inhibitor, has been shown to alleviate myocardial fibrosis and cardiac remodeling induced by myocardial infarction in mice [30]. It has been shown that the activation of NLRP3 inflammasome mediates the recruitment of inflammatory cells, particularly neutrophils, to the infarcted myocardium by releasing cytokines and chemokines [31]. Furthermore, the activation of the NLRP3 inflammasome has been shown to sustain the pro-inflammatory macrophage phenotype (M1) while inhibit the up-regulation of the pro-healing macrophage phenotype (M2), thereby prolonging the inflammatory response process [32]. Cristine J et al. have reported that the inhibition of the NLRP3 inflammasome can effectively decrease the recruitment of immune cells, reduce the proportion of M1 macrophages, and increase the proportion of M2 macrophages [26]. Our study revealed that the NLRP3 inflammasome was activated and exhibited a gradual increase within the initial 24h after reperfusion and followed by a subsequent decrease in both MIRI and EMIRI groups. Notably, the activation of the NLRP3 inflammasome in the EMIRI group was observed to be lower than that in the MIRI group at all three time points after reperfusion. By integrating the NLRP3 inflammasome activation, neutrophil infiltration, and macrophage expression, we concluded that EA preconditioning regulated neutrophil infiltration and macrophage polarization in injured myocardium via inhibiting NLRP3 inflammasome activation, promote the transition from the acute pro-inflammatory phase to the anti-inflammatory reparative phase after MIRI, ultimately resulting in a cardioprotective effect.

Myocardial ischemia results in a significant reduction in adenosine-triphosphate (ATP) levels within mitochondria, leading to glycolysis-induced lactic acid accumulation, mitochondrial swelling and dysfunction [33]. Upon restoration of blood flow, the mitochondrial respiratory chain is re-exposed to oxygen, leading to the generation of oxygen free radicals and further mitochondrial damage [33]. Following reperfusion, a significant quantity of mtDNA fragments enter to the cytoplasm, aggravating myocardial injury [34]. Perfusion of Krebs buffer containing mtDNA through coronary arteries in rats has been demonstrated to increase the size of myocardial infarction, indicating the cardiotoxic effects of mtDNA [35]. Consequently, the question arises as to how free mitochondrial DNA causes damage to the myocardium. Previous researches have shown that mtDNA serves as an endogenous agonist of the NLRP3 inflammasome [36,37]. Like bacterial DNA, mtDNA fragments are potent damage-related molecular patterns (DAMPs) recognized by TLR9 and trigger activation of NLRP3 inflammasome [38,39], blocking the cytosolic mtDNA by CsA injection or inhibiting TLR9 through E6446 intervention could decrease the expression level of NLRP3 [37]. Oka et al. have reported that mtDNA can be identified by TLR9, which subsequently triggers an inflammatory response in the myocardium, leading to the development of dilated cardiomyopathy [40]. Cyt-cyto C is a marker of mitochondrial damage, and mit-cyto C is a marker of mitochondrial integrity [41]. In the study, we evaluated the expression levels of cyt-cyto C, mit-cyto C and TLR9 in myocardial tissue, as well as the content of free mtDNA in plasma. Our findings revealed that EA preconditioning significantly upregulated the expression of mit-cyto C and downregulated the expression of cyt-cyto C and mtDNA at each time point compared to MIRI group. Additionally, the expression of TLR9 was reduced at 24h and 3d after reperfusion in the EMIRI group compared to the MIRI group. These results indicated that EA preconditioning effectively mitigated mitochondrial damage, reduced the level of plasma mtDNA, and subsequently inhibited the

activation of NLRP3 inflammasome in the myocardium after MIRI.

By integrating plasma mtDNA levels, the NLRP3 inflammasome activation, neutrophil infiltration, and macrophage expression of this study, we summarized that EA preconditioning might reduce plasma mtDNA, inhibit the activation of NLRP3 inflammasome, modulate neutrophil infiltration and macrophage polarization in the injured myocardium, facilitate the transition from the acute pro-inflammatory phase to the anti-inflammatory reparative phase after MIRI, and ultimately confer cardioprotective benefits (Fig. 6). Nonetheless, our study has some limitations. Firstly, the study primarily focused on neutrophils and macrophages to observe the impact of EA preconditioning on the dynamic changes of inflammatory response after MIRI, and future studies should explore other inflammatory immune cells. Secondly, to completely demonstrate the effect of acupuncture on TLR9 and NLRP3 inflammasome, TLR9 and NLRP3 intervention groups should be incorporated into further research. Thirdly, the precise mechanism by which EA preconditioning regulates mitochondrial damage remains unclear and requires additional investigation.

5. Conclusion

In conclusion, we found that EA preconditioning could improve the left ventricular function and reduce the size of myocardial infarction, protect the myocardium against MIRI. This beneficial effect is attributed to the modulation of dynamic inflammatory response, which is associated with the reduction of plasma mtDNA and inhibition of NLRP3 inflammasome activation. These findings may provide valuable insights into the cardioprotective mechanism of EA preconditioning.

Ethics approval and consent to participate

The authors are accountable for all aspects of the work in ensuring that questions related to the accuracy or integrity of any part of the work are appropriately investigated and resolved. This study was approved by the Animal Ethics Committee of Nanjing University of Chinese Medicine Laboratory Animal Center and was conducted in accordance with the National Institutes of Health's Guide for the Care and Use of Laboratory Animals (Permit number: 202004A009).

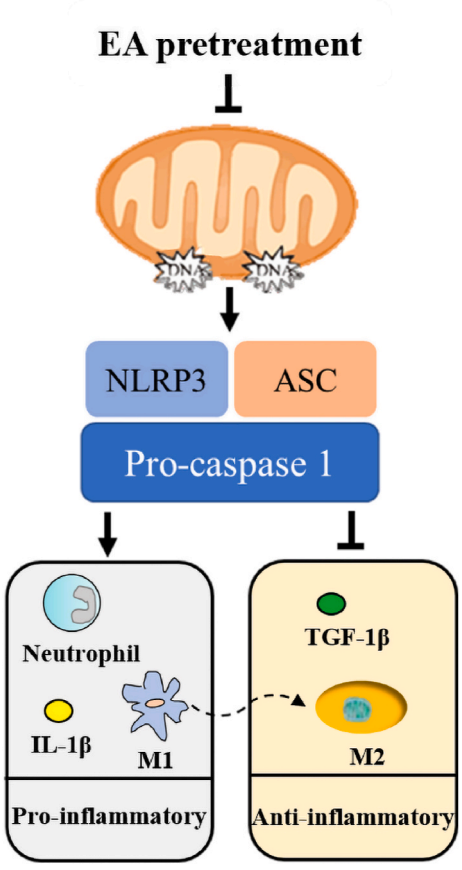

Fig. 6. Diagram of the possible mechanism for cardioprotection of EA preconditioning through inflammatory response dynamic change.

Consent for publication

We declare that the Publisher has the authors' permission to publish the relevant contribution.

Author contribution statement

Hua Bai and Senlei Xu: Conceived and designed the experiments; Analyzed and interpreted the data; Wrote the paper.

Junjing Shi, Yaping Ding, Qiongqiong Liu, Chunhong Jiang and Lili He: Performed the experiments; Analyzed and interpreted the data.

Hongru Zhang, Shengfeng Lu and Yihuang Gu: Contributed reagents, materials, analysis tools or data.

Funding statement

This study was supported by the National Natural Science Foundation of China (No.81974583, 81774210) and the Luo Linxiu Scientific Research Foundation Project of Nanjing University of Traditional Chinese Medicine (LLX202208).

Data availability statement

Data will be made available on request.

Additional information

No additional information is available for this paper.

Declaration of competing interest

The authors declare that they have no known competing financial interests or personal relationships that could have appeared to influence the work reported in this paper.

Acknowledgements

We thank Yanting Guan at Nanjing University of Chinese Medicine for the language editing.

Abbreviations

CCL2 Chemokine C–C motif ligand 2
cyto C Cytochrome *c*
cyt-cyto C Cytosolic cytochrome C
EA Electroacupuncture
EF Ejection fraction
FS Fractional shortening
IL-1β Interleukin-1β
IL-10 Interleukin-10
iNOS Induced nitric oxide synthase
LAD Left anterior descending
LV Left ventricular
MIRI Myocardial ischemia-reperfusion injury
mit-cyto C Mitochondrial cytochrome C
MPO Myeloperoxidase
mtDNA Mitochondrial deoxyribonucleic acid
NLRP3 NOD receptor family protein 3
PC6 Neiguan point
TTC 2,3, 5-triphenyltetrazolium chloride
TLR9 Toll-like receptor 9
TGF-β: Transforming growth factor-β
VEGF Vascular endothelial growth factor

References

[1] C.W. Tsao, A.W. Aday, Z.I. Almarzooq, A. Alonso, A.Z. Beaton, M.S. Bittencourt, A.K. Boehme, A.E. Buxton, A.P. Carson, Y. Commodore-Mensah, M.S.V. Elkind, K.R. Evenson, C. Eze-Nliam, J.F. Ferguson, G. Generoso, J.E. Ho, R. Kalani, S.S. Khan, B.M. Kissela, K.L. Knutson, D.A. Levine, T.T. Lewis, J. Liu, M.S. Loop, J. Ma, M.E. Mussolino, S.D. Navaneethan, A.M. Perak, R. Poudel, M. Rezk-Hanna, G.A. Roth, E.B. Schroeder, S.H. Shah, E.L. Thacker, L.B. VanWagner, S. S. Virani, J.H. Voecks, N.Y. Wang, K. Yaffe, S.S. Martin, Heart disease and stroke statistics-2022 update: a report from the American heart association, Circulation 145 (8) (2022) e153–e639, https://doi.org/10.1161/cir.0000000000001052.

[2] M. Algoet, S. Janssens, U. Himmelreich, W. Gsell, M. Pusovnik, J. Van den Eynde, W. Oosterlinck, Myocardial ischemia-reperfusion injury and the influence of inflammation, Trends Cardiovasc. Med. (2022), https://doi.org/10.1016/j.tcm.2022.02.005.

[3] S.B. Ong, S. Hernández-Reséndiz, G.E. Crespo-Avilan, R.T. Mukhametshina, X.Y. Kwek, H.A. Cabrera-Fuentes, D.J. Hausenloy, Inflammation following acute myocardial infarction: multiple players, dynamic roles, and novel therapeutic opportunities, Pharmacol. Ther. 186 (2018) 73–87, https://doi.org/10.1016/j.pharmthera.2018.01.001.

[4] G. Wei, Y. Guan, Y. Yin, J. Duan, D. Zhou, Y. Zhu, W. Quan, M. Xi, A. Wen, Anti-inflammatory effect of protocatechuic aldehyde on myocardial ischemia/reperfusion injury in vivo and in vitro, Inflammation 36 (3) (2013) 592–602, https://doi.org/10.1007/s10753-012-9581-z.

[5] M. Hou, X. Wu, Z. Zhao, Q. Deng, Y. Chen, L. Yin, Endothelial cell-targeting, ROS-ultrasensitive drug/siRNA co-delivery nanocomplexes mitigate early-stage neutrophil recruitment for the anti-inflammatory treatment of myocardial ischemia reperfusion injury, Acta Biomater. 143 (2022) 344–355, https://doi.org/10.1016/j.actbio.2022.02.018.

[6] I. Andreadou, H.A. Cabrera-Fuentes, Y. Devaux, N.G. Frangogiannis, S. Frantz, T. Guzik, E.A. Liehn, C.P.C. Gomes, R. Schulz, D.J. Hausenloy, Immune cells as targets for cardioprotection: new players and novel therapeutic opportunities, Cardiovasc. Res. 115 (7) (2019) 1117–1130, https://doi.org/10.1093/cvr/cvz050.

[7] D.L. Mann, The emerging role of innate immunity in the heart and vascular system: for whom the cell tolls, Circ. Res. 108 (9) (2011) 1133–1145, https://doi.org/10.1161/circresaha.110.226936.

[8] S. Willenborg, T. Lucas, G. van Loo, J.A. Knipper, T. Krieg, I. Haase, B. Brachvogel, M. Hammerschmidt, A. Nagy, N. Ferrara, M. Pasparakis, S.A. Eming, CCR2 recruits an inflammatory macrophage subpopulation critical for angiogenesis in tissue repair, Blood 120 (3) (2012) 613–625, https://doi.org/10.1182/blood-2012-01-403386.

[9] M. Nahrendorf, F.K. Swirski, Monocyte and macrophage heterogeneity in the heart, Circ. Res. 112 (12) (2013) 1624–1633, https://doi.org/10.1161/circresaha.113.300890.

[10] Y. Jing, F. Wu, D. Li, L. Yang, Q. Li, R. Li, Metformin improves obesity-associated inflammation by altering macrophages polarization, Mol. Cell. Endocrinol. 461 (2018) 256–264, https://doi.org/10.1016/j.mce.2017.09.025.

[11] L. Zhao, D. Li, H. Zheng, X. Chang, J. Cui, R. Wang, J. Shi, H. Fan, Y. Li, X. Sun, F. Zhang, X. Wu, F. Liang, Acupuncture as adjunctive therapy for chronic stable angina: a randomized clinical trial, JAMA Intern. Med. 179 (10) (2019) 1388–1397, https://doi.org/10.1001/jamainternmed.2019.2407.

[12] Y.F. Song, L.X. Pei, L. Chen, H. Geng, M.Q. Yuan, W.L. Xu, J. Wu, J.Y. Zhou, J.H. Sun, Electroacupuncture relieves irritable bowel syndrome by regulating IL-18 and gut microbial dysbiosis in a trinitrobenzene sulfonic acid-induced post-inflammatory animal model, Am. J. Chin. Med. 48 (1) (2020) 77–90, https://doi.org/10.1142/s0192415x20500044.

[13] X. Wang, N.Q. Zhao, Y.X. Sun, X. Bai, J.T. Si, J.P. Liu, Z.L. Liu, Acupuncture for ulcerative colitis: a systematic review and meta-analysis of randomized clinical trials, BMC Complement Med Ther 20 (1) (2020) 309, https://doi.org/10.1186/s12906-020-03101-4.

[14] S. Liu, Z.F. Wang, Y.S. Su, R.S. Ray, X.H. Jing, Y.Q. Wang, Q. Ma, Somatotopic organization and intensity dependence in driving distinct NPY-expressing sympathetic pathways by electroacupuncture, Neuron 108 (3) (2020) 436–450.e7, https://doi.org/10.1016/j.neuron.2020.07.015.

[15] T. Zhang, W.X. Yang, Y.L. Wang, J. Yuan, Y. Qian, Q.M. Sun, M.L. Yu, S.P. Fu, B. Xu, S.F. Lu, Electroacupuncture preconditioning attenuates acute myocardial ischemia injury through inhibiting NLRP3 inflammasome activation in mice, Life Sci. 248 (2020), 117451, https://doi.org/10.1016/j.lfs.2020.117451.

[16] X.F. Xia, Y.C. Liu, S.F. Lu, H. Bai, S.L. Xu, K. Sun, J.H. Wu, Y.H. Gu, H.R. Zhang, [Effect of electroacupuncture preconditioning on expression of Gasdermin D, Caspase-1 and IL-1β in rats with myocardial ischemia reperfusion injury], Zhen Ci Yan Jiu 47 (5) (2022) 443–448, https://doi.org/10.13702/j.1000-0607.20210286.

[17] W. Chen, Z. Zhong, H. Bai, H. Zhang, S. Lu, Y. Gu, [An autophagic mechanism study on effect of electroacupuncture at different times pretreating myocardial ischemia-reperfusion injury], Zhongguo Zhen Jiu 38 (10) (2018) 1087–1092, https://doi.org/10.13703/j.0255-2930.2018.10.015.

[18] Y. Xiao, W. Chen, Z. Zhong, L. Ding, H. Bai, H. Chen, H. Zhang, Y. Gu, S. Lu, Electroacupuncture preconditioning attenuates myocardial ischemia-reperfusion injury by inhibiting mitophagy mediated by the mTORC1-ULK1-FUNDC1 pathway, Biomed. Pharmacother. 127 (2020), 110148, https://doi.org/10.1016/j.biopha.2020.110148.

[19] H.R. Zhang, J.L. Tao, H. Bai, E.M. Yang, Z.H. Zhong, X.T. Liu, Y.H. Gu, S.F. Lu, Changes in the serum metabolome of acute myocardial ischemia rat pretreatment with electroacupuncture, Am. J. Chin. Med. 47 (5) (2019) 1025–1041, https://doi.org/10.1142/s0192415x19500526.

[20] H. Bai, K. Sun, J.H. Wu, Z.H. Zhong, S.L. Xu, H.R. Zhang, Y.H. Gu, S.F. Lu, Proteomic and metabolomic characterization of cardiac tissue in acute myocardial ischemia injury rats, PLoS One 15 (5) (2020), e0231797, https://doi.org/10.1371/journal.pone.0231797.

[21] K. Tajiri, K. Imanaka-Yoshida, A. Matsubara, Y. Tsujimura, M. Hiroe, T. Naka, N. Shimojo, S. Sakai, K. Aonuma, Y. Yasutomi, Suppressor of cytokine signaling 1 DNA administration inhibits inflammatory and pathogenic responses in autoimmune myocarditis, J. Immunol. 189 (4) (2012) 2043–2053, https://doi.org/10.4049/jimmunol.1103610.

[22] S. Dogan, V. Vasudevaraja, B. Xu, J. Serrano, R.N. Ptashkin, H.J. Jung, S. Chiang, A.A. Jungbluth, M.A. Cohen, I. Ganly, M.F. Berger, A. Momeni Boroujeni, R. A. Ghossein, M. Ladanyi, D.J. Chute, M. Snuderl, DNA methylation-based classification of sinonasal undifferentiated carcinoma, Mod. Pathol. 32 (10) (2019) 1447–1459, https://doi.org/10.1038/s41379-019-0285-x.

[23] S. Chen, H. Chen, Q. Du, J. Shen, Targeting myeloperoxidase (MPO) mediated oxidative stress and inflammation for reducing brain ischemia injury: potential application of natural compounds, Front. Physiol. 11 (2020) 433, https://doi.org/10.3389/fphys.2020.00433.

[24] R.A. Kloner, D.A. Brown, M. Csete, W. Dai, J.M. Downey, R.A. Gottlieb, S.L. Hale, J. Shi, New and revisited approaches to preserving the reperfused myocardium, Nat. Rev. Cardiol. 14 (11) (2017) 679–693, https://doi.org/10.1038/nrcardio.2017.102.

[25] V. Rusinkevich, Y. Huang, Z.Y. Chen, W. Qiang, Y.G. Wang, Y.F. Shi, H.T. Yang, Temporal dynamics of immune response following prolonged myocardial ischemia/reperfusion with and without cyclosporine A, Acta Pharmacol. Sin. 40 (9) (2019) 1168–1183, https://doi.org/10.1038/s41401-018-0197-1.

[26] C.J. Reitz, F.J. Alibhai, T.N. Khatua, M. Rasouli, B.W. Bridle, T.P. Burris, T.A. Martino, SR9009 administered for one day after myocardial ischemia-reperfusion prevents heart failure in mice by targeting the cardiac inflammasome, Commun. Biol. 2 (2019) 353, https://doi.org/10.1038/s42003-019-0595-z.

[27] Z.Q. Zhao, D.A. Velez, N.P. Wang, K.O. Hewan-Lowe, M. Nakamura, R.A. Guyton, J. Vinten-Johansen, Progressively developed myocardial apoptotic cell death during late phase of reperfusion, Apoptosis 6 (4) (2001) 279–290, https://doi.org/10.1023/a:1011335525219.

[28] N. Kelley, D. Jeltema, Y. Duan, Y. He, The NLRP3 inflammasome: an overview of mechanisms of activation and regulation, Int. J. Mol. Sci. 20 (13) (2019) 3328, https://doi.org/10.3390/ijms20133328.

[29] Y.W. Yu, J.Q. Que, S. Liu, K.Y. Huang, L. Qian, Y.B. Weng, F.N. Rong, L. Wang, Y.Y. Zhou, Y.J. Xue, K.T. Ji, Sodium-glucose Co-transporter-2 inhibitor of dapagliflozin attenuates myocardial ischemia/reperfusion injury by limiting NLRP3 inflammasome activation and modulating autophagy, Front Cardiovasc Med 8 (2021), 768214, https://doi.org/10.3389/fcvm.2021.768214.

[30] R.F. Gao, X. Li, H.Y. Xiang, H. Yang, C.Y. Lv, X.L. Sun, H.Z. Chen, Y. Gao, J.S. Yang, W. Luo, Y.Q. Yang, Y.H. Tang, The covalent NLRP3-inflammasome inhibitor Oridonin relieves myocardial infarction induced myocardial fibrosis and cardiac remodeling in mice, Int. Immunopharm. 90 (2021), 107133, https://doi.org/10.1016/j.intimp.2020.107133.

[31] X. Tian, H. Sun, A.J. Casbon, E. Lim, K.P. Francis, J. Hellman, A. Prakash, NLRP3 inflammasome mediates dormant neutrophil recruitment following sterile lung injury and protects against subsequent bacterial pneumonia in mice, Front. Immunol. 8 (2017) 1337, https://doi.org/10.3389/fimmu.2017.01337.

[32] J. Zhang, X. Liu, C. Wan, Y. Liu, Y. Wang, C. Meng, Y. Zhang, C. Jiang, NLRP3 inflammasome mediates M1 macrophage polarization and IL-1β production in inflammatory root resorption, J. Clin. Periodontol. 47 (4) (2020) 451–460, https://doi.org/10.1111/jcpe.13258.
[33] E.J. Lesnefsky, Q. Chen, B. Tandler, C.L. Hoppel, Mitochondrial dysfunction and myocardial ischemia-reperfusion: implications for novel therapies, Annu. Rev. Pharmacol. Toxicol. 57 (2017) 535–565, https://doi.org/10.1146/annurev-pharmtox-010715-103335.
[34] N. García, E. Chávez, Mitochondrial DNA fragments released through the permeability transition pore correspond to specific gene size, Life Sci. 81 (14) (2007) 1160–1166, https://doi.org/10.1016/j.lfs.2007.08.019.
[35] X.M. Yang, L. Cui, J. White, J. Kuck, M.V. Ruchko, G.L. Wilson, M. Alexeyev, M.N. Gillespie, J.M. Downey, M.V. Cohen, Mitochondrially targeted Endonuclease III has a powerful anti-infarct effect in an in vivo rat model of myocardial ischemia/reperfusion, Basic Res. Cardiol. 110 (2) (2015) 3, https://doi.org/10.1007/s00395-014-0459-0.
[36] G.A. Ward, R.P. Dalton 3rd, B.S. Meyer, A.F. McLemore, A.L. Aldrich, N.B. Lam, A.H. Onimus, N.D. Vincelette, T.L. Trinh, X. Chen, A.R. Calescibetta, S. M. Christiansen, H.A. Hou, J.O. Johnson, K.L. Wright, E. Padron, E.A. Eksioglu, A.F. List, Oxidized mitochondrial DNA engages TLR9 to activate the NLRP3 inflammasome in myelodysplastic syndromes, Int. J. Mol. Sci. 24 (4) (2023), https://doi.org/10.3390/ijms24043896.
[37] P. Lu, H. Zheng, H. Meng, C. Liu, L. Duan, J. Zhang, Z. Zhang, J. Gao, Y. Zhang, T. Sun, Mitochondrial DNA induces nucleus pulposus cell pyroptosis via the TLR9-NF-κB-NLRP3 axis, J. Transl. Med. 21 (1) (2023) 389, https://doi.org/10.1186/s12967-023-04266-5.
[38] D. Arnoult, F. Soares, I. Tattoli, S.E. Girardin, Mitochondria in innate immunity, EMBO Rep. 12 (9) (2011) 901–910, https://doi.org/10.1038/embor.2011.157.
[39] Q. Zhang, M. Raoof, Y. Chen, Y. Sumi, T. Sursal, W. Junger, K. Brohi, K. Itagaki, C.J. Hauser, Circulating mitochondrial DAMPs cause inflammatory responses to injury, Nature 464 (7285) (2010) 104–107, https://doi.org/10.1038/nature08780.
[40] T. Oka, S. Hikoso, O. Yamaguchi, M. Taneike, T. Takeda, T. Tamai, J. Oyabu, T. Murakawa, H. Nakayama, K. Nishida, S. Akira, A. Yamamoto, I. Komuro, K. Otsu, Mitochondrial DNA that escapes from autophagy causes inflammation and heart failure, Nature 485 (7397) (2012) 251–255, https://doi.org/10.1038/nature10992.
[41] F.Y. Lee, P.L. Shao, C.G. Wallace, S. Chua, P.H. Sung, S.F. Ko, H.T. Chai, S.Y. Chung, K.H. Chen, H.I. Lu, Y.L. Chen, T.H. Huang, J.J. Sheu, H.K. Yip, Combined therapy with SS31 and mitochondria mitigates myocardial ischemia-reperfusion injury in rats, Int. J. Mol. Sci. 19 (9) (2018) 2782, https://doi.org/10.3390/ijms19092782.